

Supporting information

ELECTROCHEMICAL STUDIES OF A NOVEL BIS (HYDRAZONE) LIGAND AND ITS GRID COMPLEX

Figure S 1. ^1H -NMR (CDCl_3 , 400MHz) spectrum of 2-(4-butylphenyl)-4,6-dichloropyrimidine (1).	2
Figure S 2. ^{13}C -NMR ($\text{DMSO}-d_6$, 101 MHz) spectrum of 2-(4-butylphenyl)-4,6- dihydrazinylpyrimidine (2).	2
Figure S 3. ^1H NMR of compounds 2 (400MHz, $\text{DMSO}-d_6$) and 3 (400MHz, CDCl_3).	3
Figure S 4. ^1H -NMR- NOESY of compound 3 (400 MHz, CDCl_3).	3
Figure S 5. 2D-NMR COSY($\text{DMSO}-d_6$, 400 MHz) spectrum of the 2-(4-butylphenyl)-4,6-dihydrazinylpyrimidine (2) aromatic region onset.	4
Figure S 6. 2D-NMR COSY ($\text{DMSO}-d_6$, 400 MHz) spectrum of the 2-(4-butylphenyl)-4,6-dihydrazinylpyrimidine (2) Aliphatic region onset.	4
Figure S 7. 2D-NMR HSQC ($\text{DMSO}-d_6$, 400 MHz) of the 2-(4-butylphenyl)-4,6- dihydrazinylpyrimidine (2) aromatic region onset.	5
Figure S 8. 2D-NMR HSQC ($\text{DMSO}-d_6$, 400 MHz) of the 2-(4-butylphenyl)-4,6- dihydrazinylpyrimidine (2) Aliphatic region onset.	5
Figure S 9. ^{13}C -NMR (CDCl_3 , 101 MHz) spectrum of Bis(hydrazone) 3	6
Figure S 10. 2D-NMR COSY (CDCl_3 , 400 MHz) spectrum of Bis(hydrazone) 3 . Aromatic region onset... 6	6
Figure S 11. 2D-NMR COSY (CDCl_3 , 400 MHz) spectrum of Bis(hydrazone) 3 . Aliphatic region onset... 7	7
Figure S 12. 2D-NMR HSQC (CDCl_3 , 400 MHz) spectrum of Bis(hydrazone) 3	7
Figure S 13. 2D-NMR COSY ($\text{CD}_3\text{CN}-d_3$, 400 MHz) of grid complex $[\text{Zn}_4 \text{L}_4] \cdot 8(\text{BF}_4)$. Aromatic region onset	8
Figure S 14. 2D-NMR COSY ($\text{CD}_3\text{CN}-d_3$, 400 MHz) of grid complex $[\text{Zn}_4 \text{L}_4] \cdot 8(\text{BF}_4)$. Aliphatic region onset.....	8
Figure S 15. 2D-NMR NOESY ($\text{CD}_3\text{CN}-d_3$, 400 MHz) of grid complex $[\text{Zn}_4 \text{L}_4] \cdot 8(\text{BF}_4)$. Aliphatic region onset.....	9
Figure S 16 UV-Vis Spectra of ligand 3 and Grid like complex $[(\text{Zn}_4(3)_4)] (\text{BF}_4)_8$ in methanol.	9
Figure S 17. Randles-Sevick linear fit for oxidation peaks in (a) bis(hydrazone) (3) and (B) grid complex $[\text{Zn}_4 \text{L}_4] \cdot 8(\text{BF}_4)$	10
Figure S 18. Randles-Sevick linear fit for oxidation peaks in (a) bis(hydrazone) (3) and (B) grid complex $[\text{Zn}_4 \text{L}_4] \cdot 8(\text{BF}_4)$	11

NMR ANALYSIS.

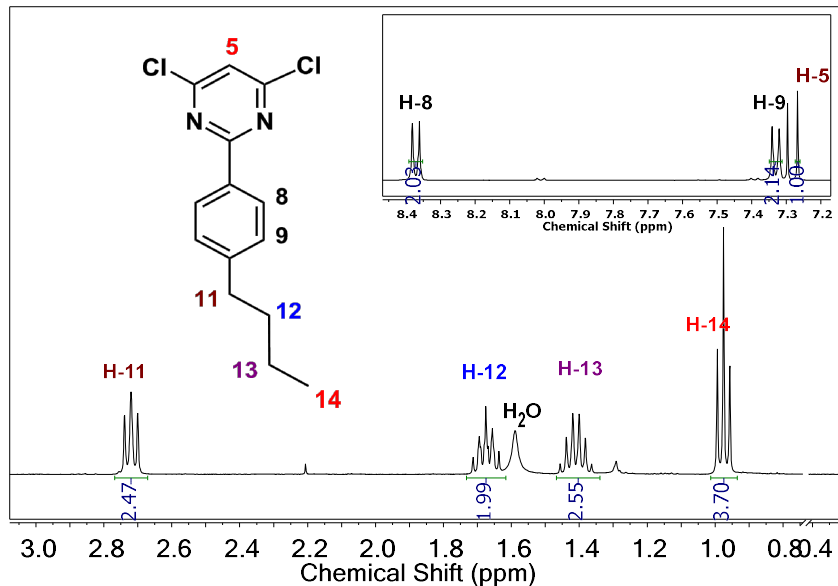


Figure S 1 ¹H-NMR (CDCl_3 , 400MHz) spectrum of 2-(4-butylphenyl)-4,6-dichloropyrimidine (1).

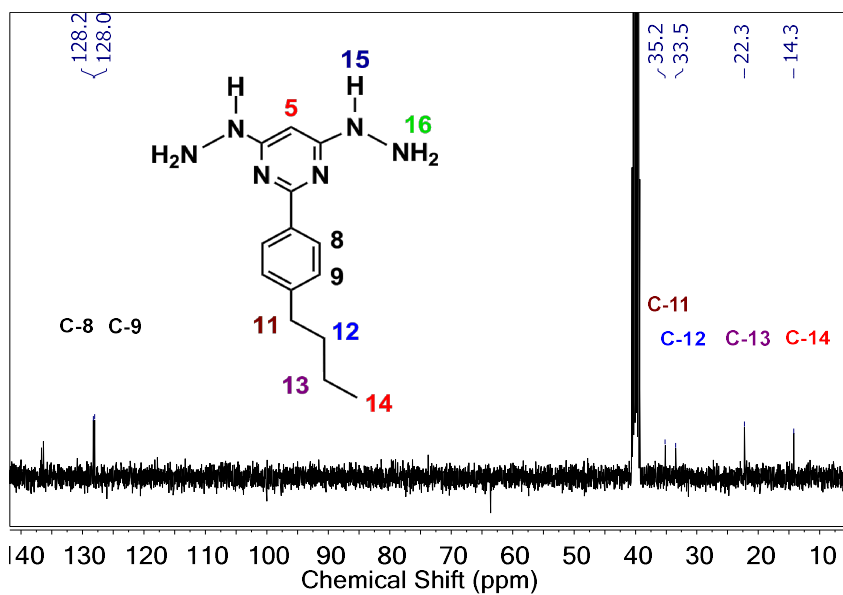


Figure S 2 ¹³C-NMR ($\text{DMSO}-d_6$, 101 MHz) spectrum of 2-(4-butylphenyl)-4,6-dihydrazinylpyrimidine (2).

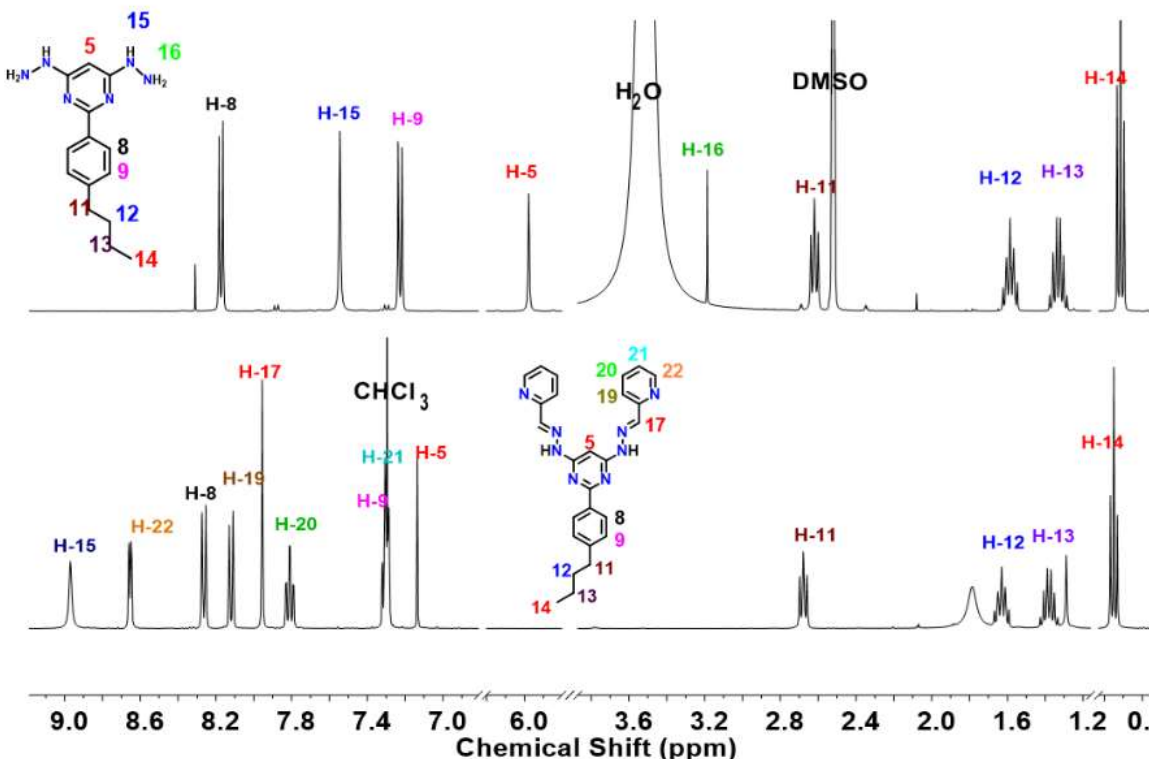


Figure S 3. ^1H NMR of compounds **2** (400MHz, $\text{DMSO}-d_6$) and **3** (400MHz, CDCl_3).

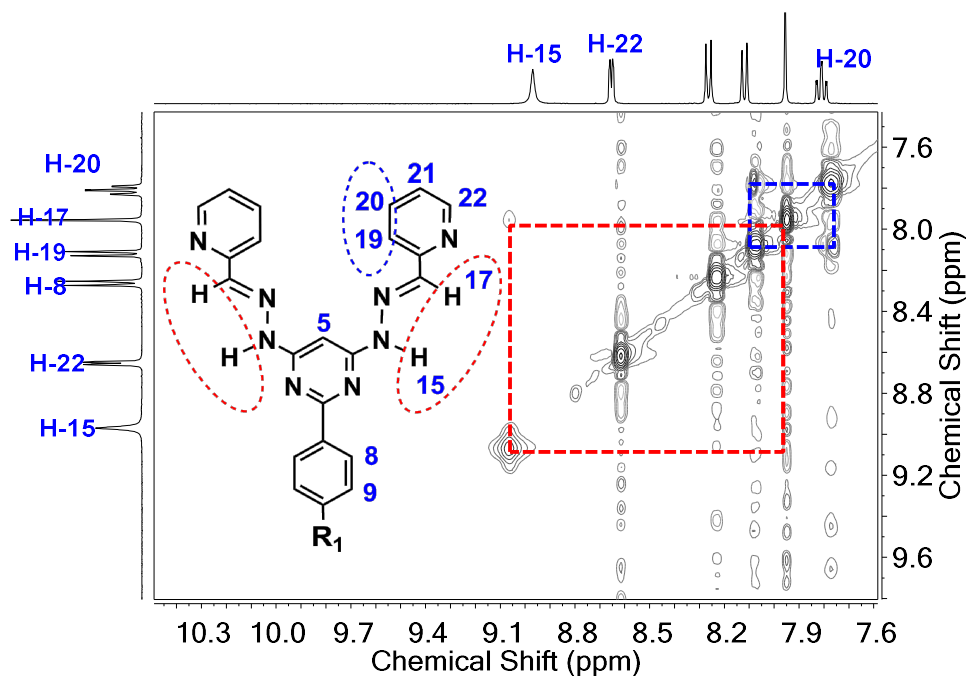


Figure S 4. ^1H -NMR- NOESY of compound **3** (400 MHz, CDCl_3).

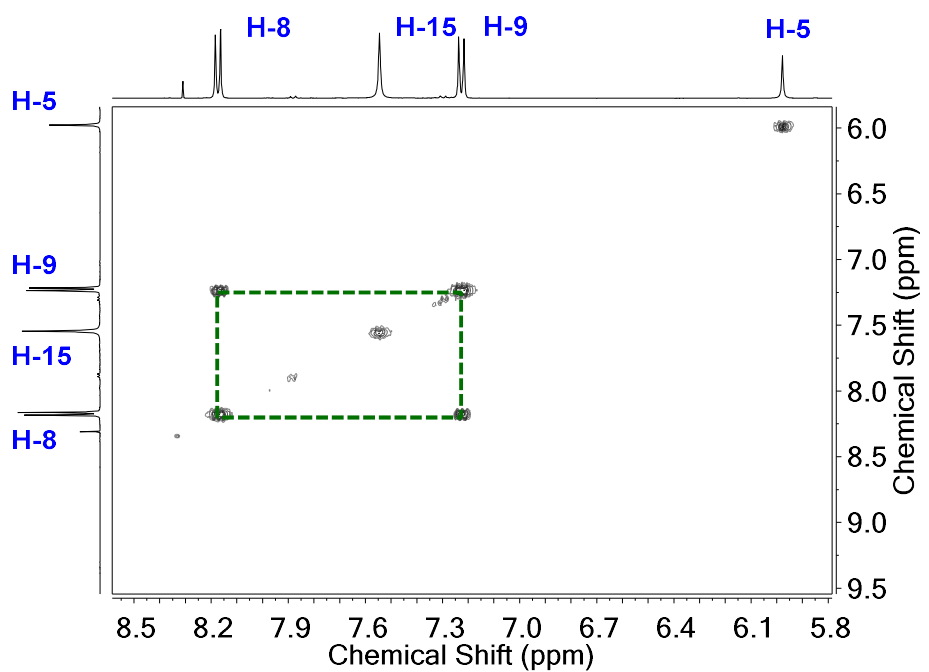


Figure S 5. 2D-NMR COSY(DMSO-*d*₆, 400 MHz) spectrum of the 2-(4-butylphenyl)-4,6- dihydrazinylpyrimidine (2) aromatic region onset.

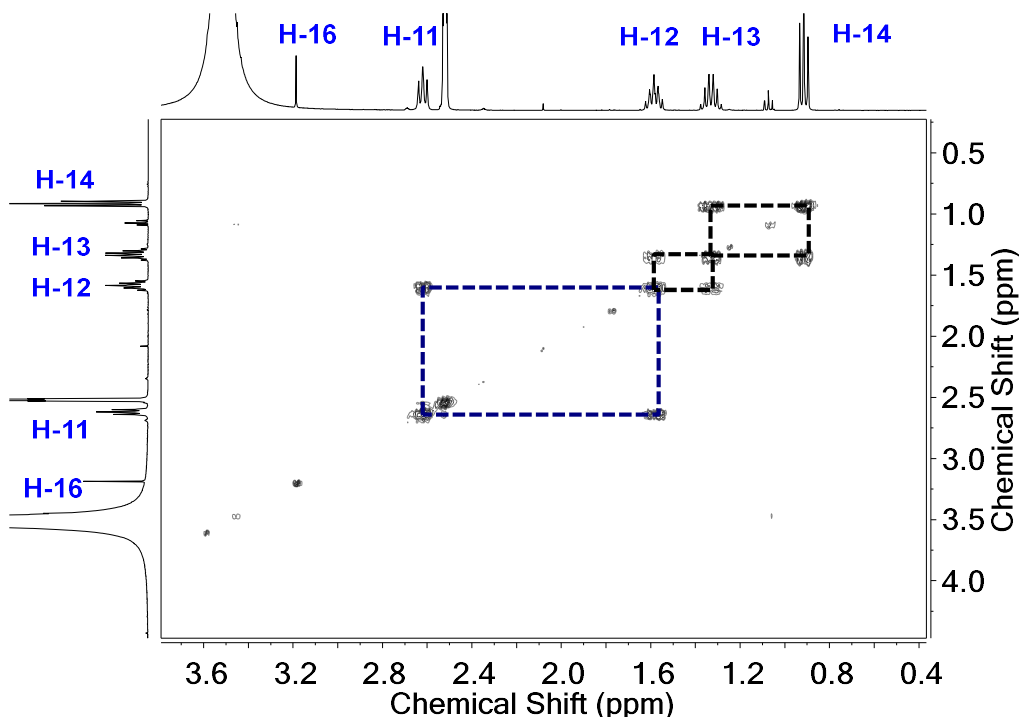


Figure S 6. 2D-NMR COSY (DMSO-*d*₆, 400 MHz) spectrum of the 2-(4-butylphenyl)-4,6- dihydrazinylpyrimidine (2) Aliphatic region onset.

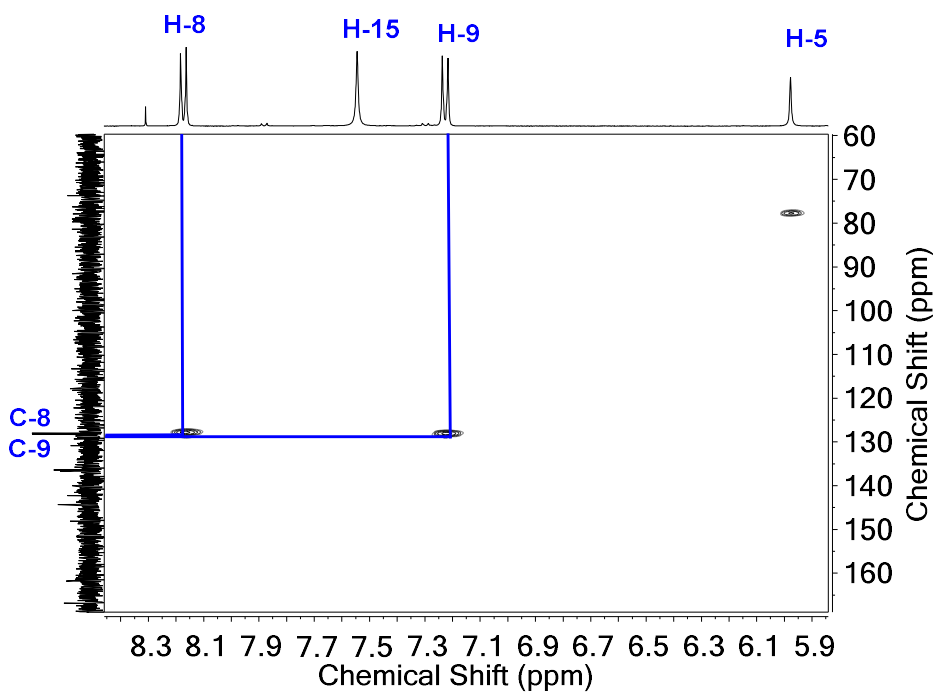


Figure S 7. 2D-NMR HSQC (DMSO-*d*₆, 400 MHz) of the 2-(4-butylphenyl)-4,6- dihydrazinylpyrimidine (2) aromatic region onset.

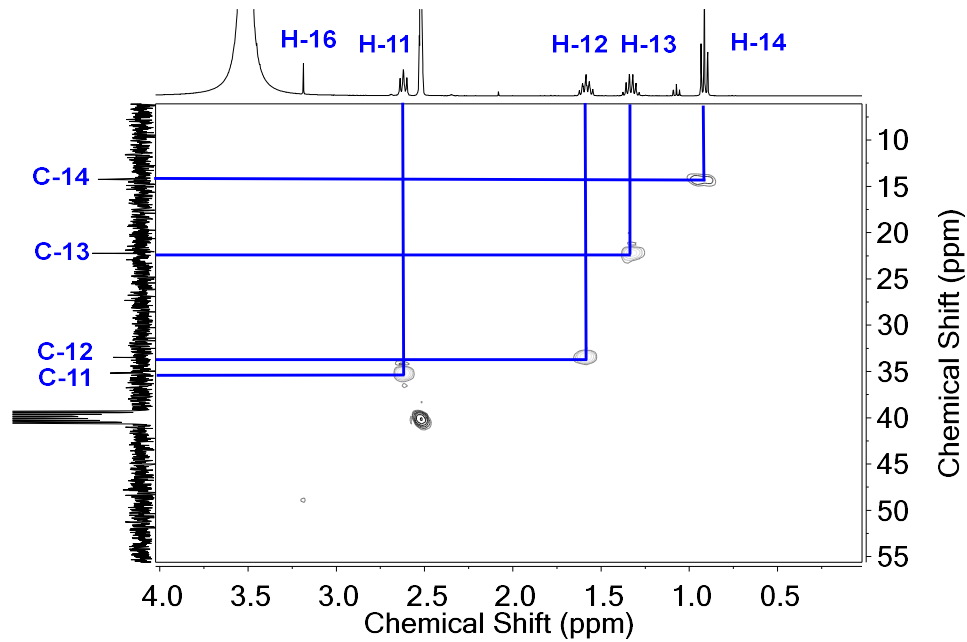


Figure S 8. 2D-NMR HSQC (DMSO-*d*₆, 400 MHz) of the 2-(4-butylphenyl)-4,6- dihydrazinylpyrimidine (2) Aliphatic region onset.

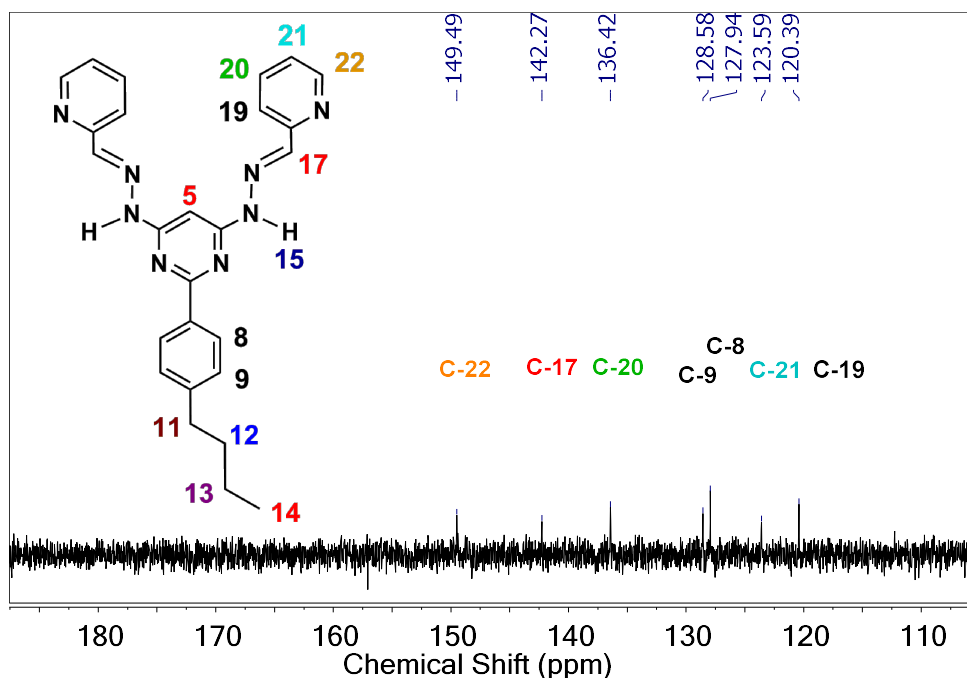


Figure S 9. ^{13}C -NMR (CDCl_3 , 101 MHz) spectrum of Bis(hydrazone) 3.

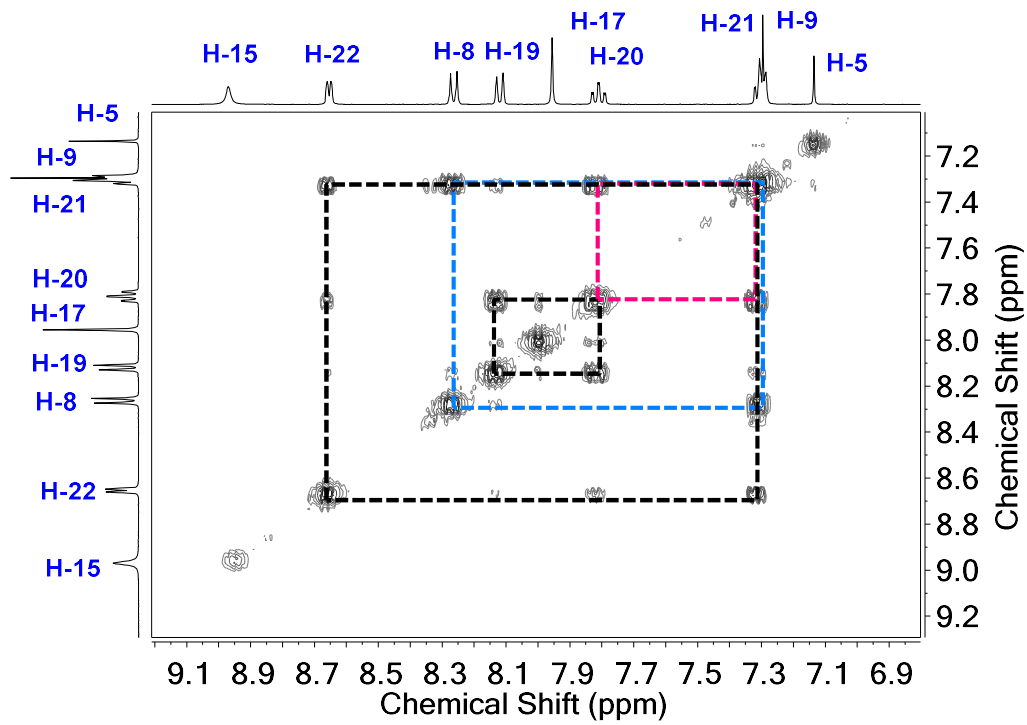


Figure S 10. 2D-NMR COSY (CDCl_3 , 400 MHz) spectrum of Bis(hydrazone) 3. Aromatic region onset.

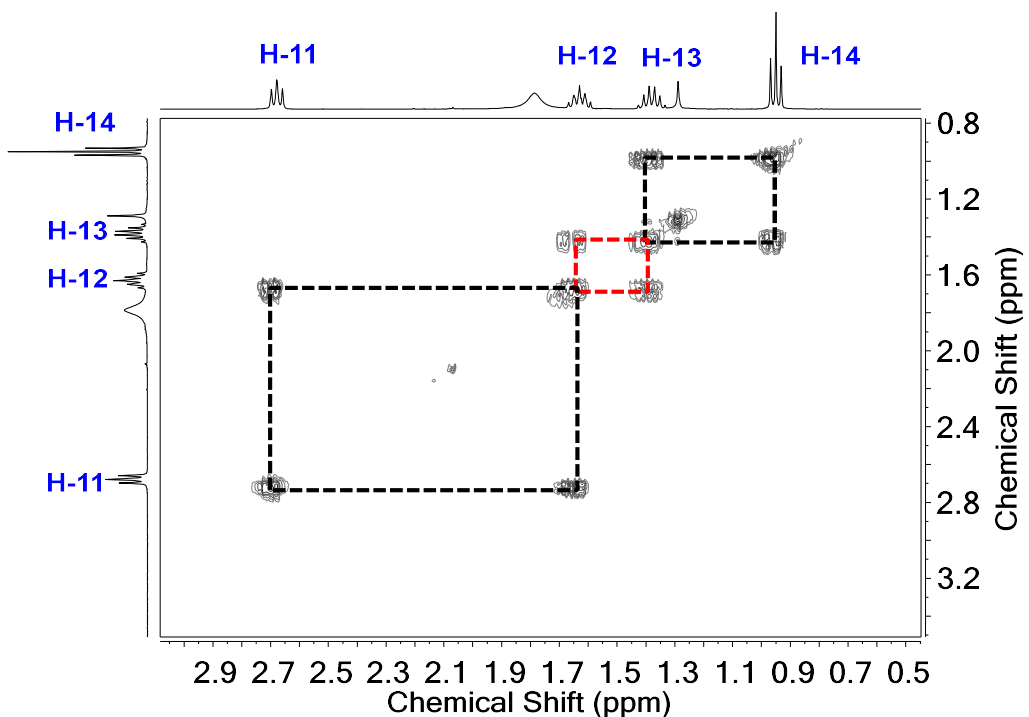


Figure S 11. 2D-NMR COSY (CDCl_3 , 400 MHz) spectrum of Bis(hydrazone) 3. Aliphatic region onset.

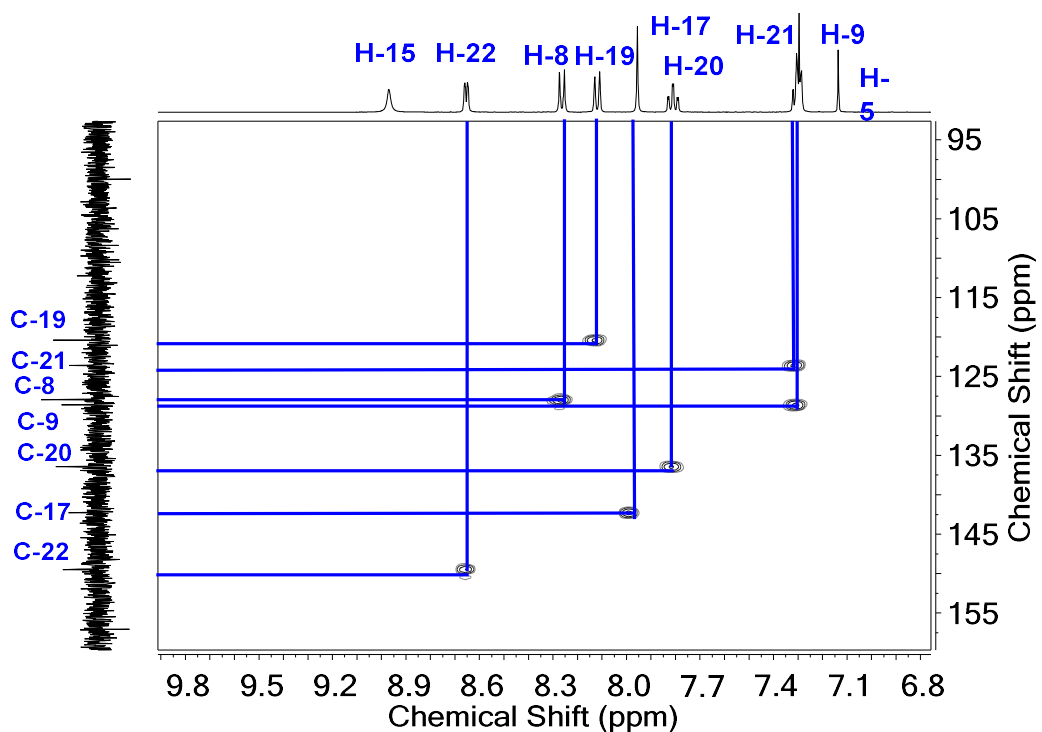


Figure S 12. 2D-NMR HSQC (CDCl_3 , 400 MHz) spectrum of Bis(hydrazone) 3.

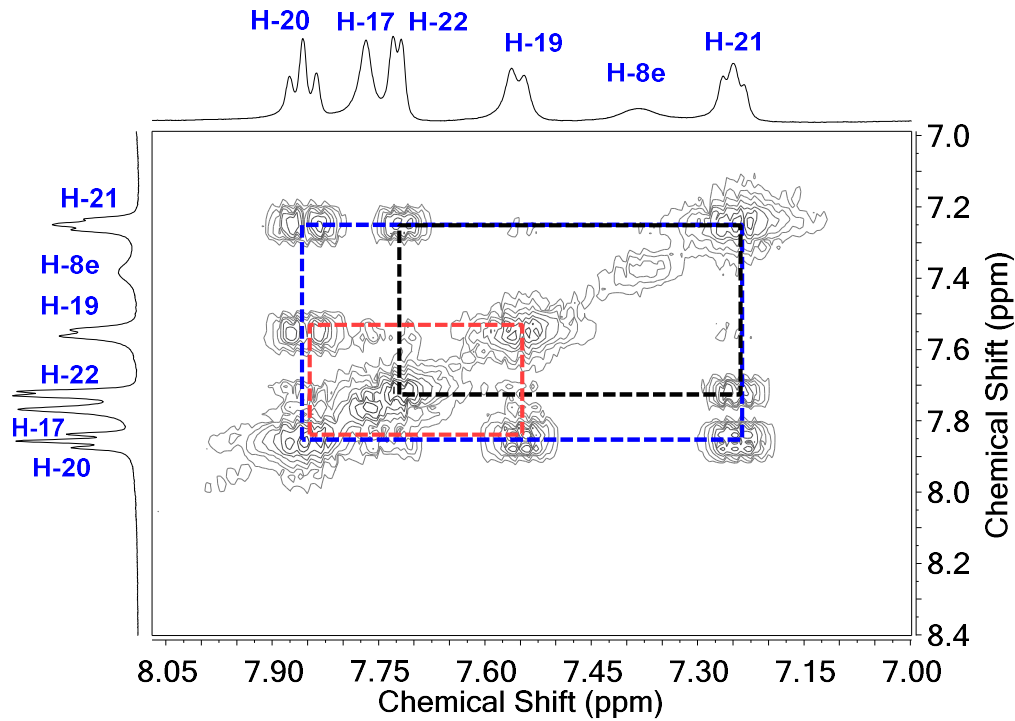


Figure S 13. 2D-NMR COSY ($\text{CD}_3\text{CN}-d_3$, 400 MHz) of grid complex $[\text{Zn}_4 \text{L}_4] \cdot 8(\text{BF}_4)$. Aromatic region onset .

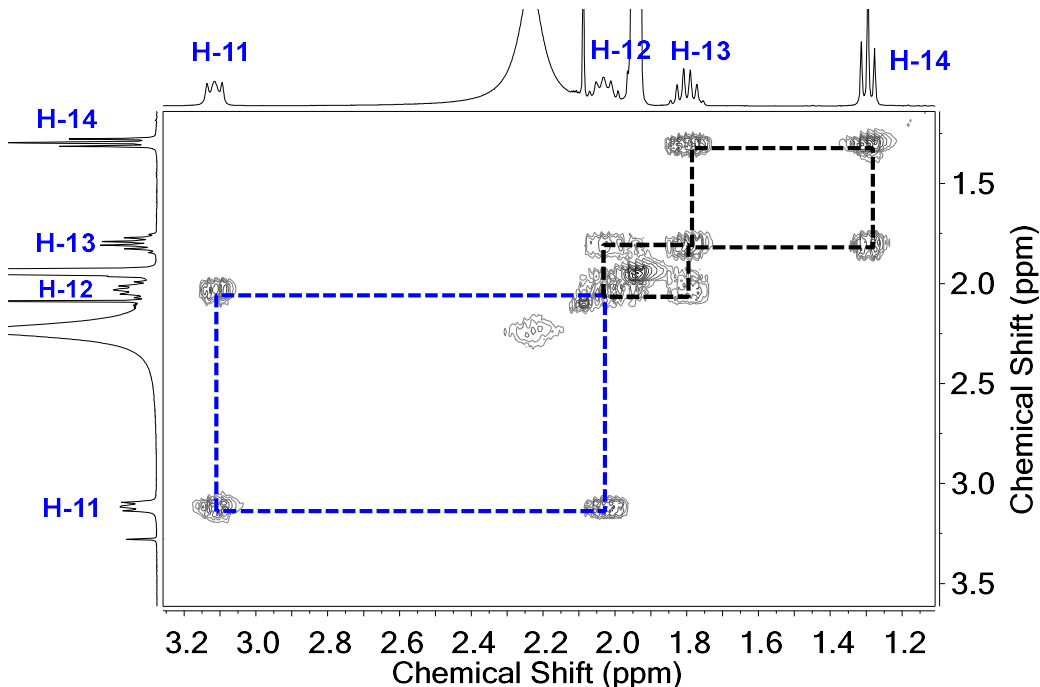


Figure S 14. 2D-NMR COSY ($\text{CD}_3\text{CN}-d_3$, 400 MHz) of grid complex $[\text{Zn}_4 \text{L}_4] \cdot 8(\text{BF}_4)$. Aliphatic region onset.

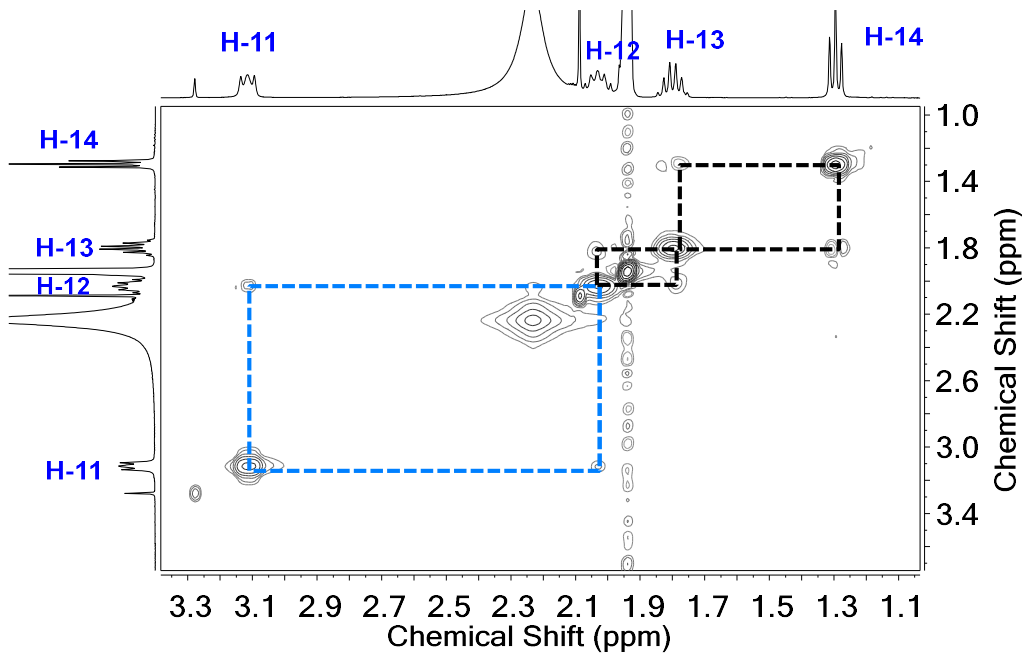


Figure S 15. 2D-NMR NOESY ($\text{CD}_3\text{CN}-d_3$, 400 MHz) of grid complex $[\text{Zn}_4 \text{L}_4] \cdot 8(\text{BF}_4)$. Aliphatic region onset.

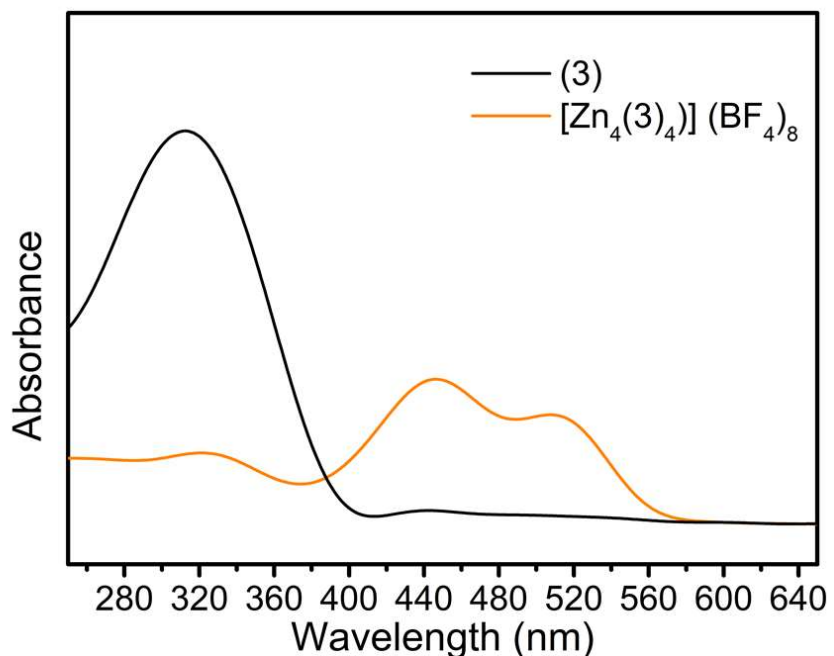


Figure S 16 UV-Vis Spectra of ligand **3** and Grid like complex $[\text{Zn}_4(3)_4](\text{BF}_4)_8$ in methanol.

Electrochemical Analysis

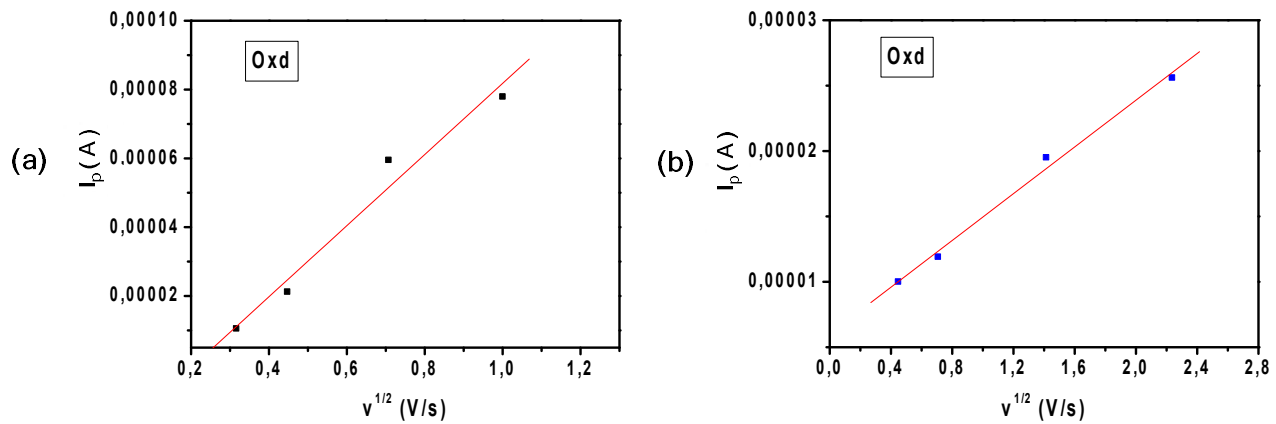


Figure S 17. Randless-Sevick linear fit for oxidation peaks in (a) bis(hydrazone) (3) and (B) grid complex $[\text{Zn}_4 \text{L}_4] \cdot 8(\text{BF}_4)$

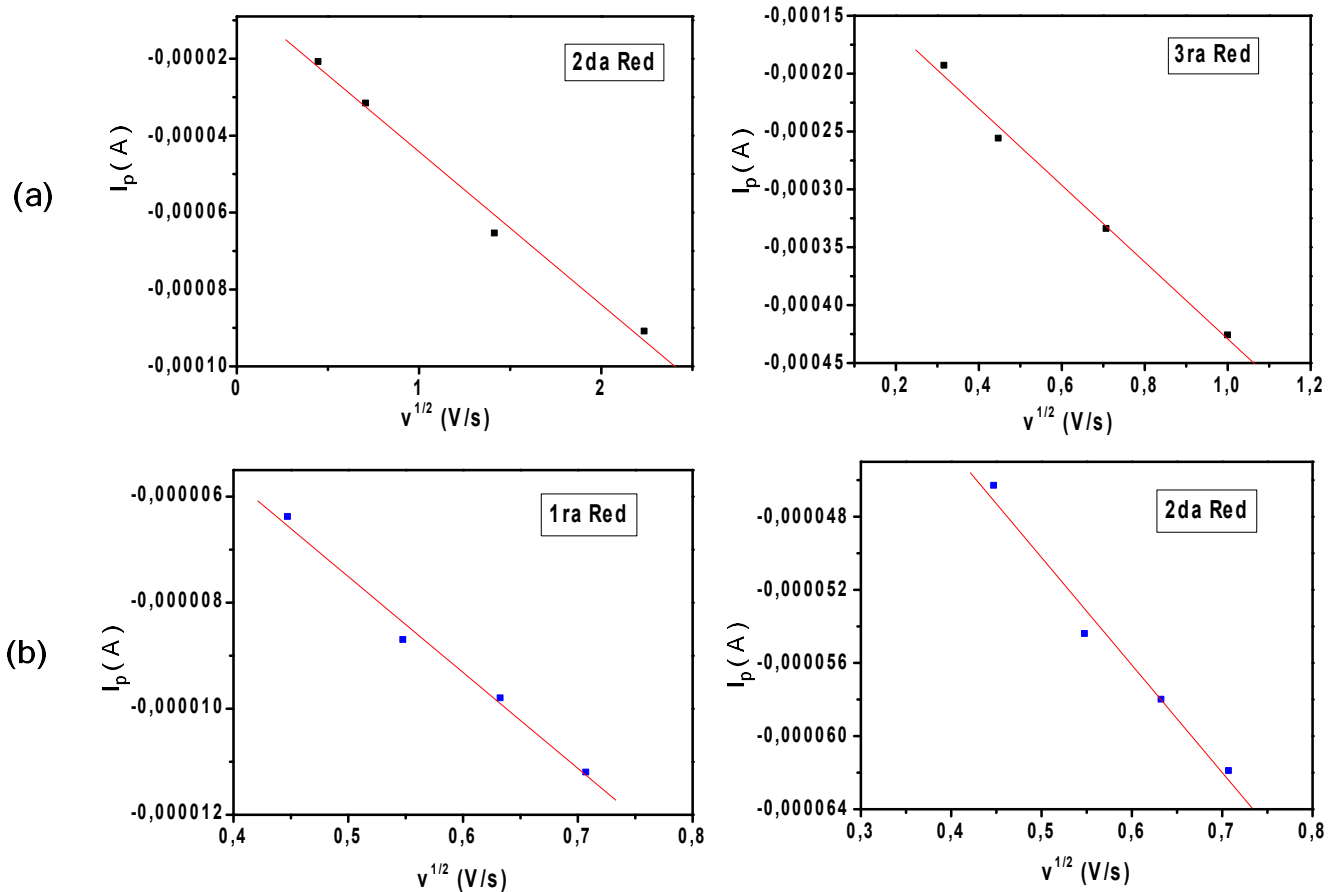


Figure S 18. Randless-Sevick linear fit for oxidation peaks in (a) bis(hydrazone) (3) and (B) grid complex $[\text{Zn}_4 \text{L}_4] \cdot 8(\text{BF}_4)$